Frontiers in Health Informatics
ISSN-Online: 2676-7104
www.healthinformaticsjournal.com
2024; 13: 07
Open Access

Preparation, Characterization and Cytotoxicity Evaluation of Curcuminoid Compound Loaded PLGA Nanoparticles for Chemotherapy of Cancer

J. Sangeetha[1], Mubeen G[2], Parameswari Prabhu[3*], Arman Dalal[4], Deblina Sardar[5], Shiv Kumar Sharma[6], Himanshu Panchal[7], Twinkle Kumari[8]

[1]Department of Pharmacognosy, Mallareddy institute of Pharmaceutical Sciences, Maisammaguda, Dhulapally, kompally, Secunderabad -500100.
[2]Department of Pharmaceutical Quality Assurance, Al-Ameen College of Pharmacy, Hosur Road, Bangalore, India Pin- 560027.
[3*]Department of Pharmaceutics, Mohammed Sathak AJ College of Pharmacy Medavakkam Road, Sholinganallur, Chennai, Tamil Nadu Pin-600119.
[4]Institute of Pharmaceutical Research, GLA University, Mathura - Delhi Road, Chaumuhan, Mathura - 281406, Uttar Pradesh, India.
[5]Department of Pharmacology, Eminent College of Pharmaceutical Technology, Barasat, Kolkata, West Bengal, India Pin- 700126.
[6,7,8]Department of Pharmacology, HRIT University, Morta, Ghaziabad, Uttar Pradesh 201003.
Corresponding Author: Parameswari Prabhu, Department of Pharmaceutics, Mohammed Sathak AJ College of Pharmacy Medavakkam Road, Sholinganallur, Chennai, Tamil Nadu Pin-600119.

Cite this paper as: J. Sangeetha, Mubeen G, Parameswari Prabhu, Arman Dalal, Deblina Sardar, Shiv Kumar Sharma, Himanshu Panchal, Twinkle Kumari (2024). Preparation, Characterization and Cytotoxicity Evaluation of Curcuminoid Compound Loaded PLGA Nanoparticles for Chemotherapy of Cancer. *Frontiers in Health Informatics, 13 (7) 254-267*

A B S T R A C T

The current study aimed to evaluate the formulation, characterization, and in vitro drug release properties of polymeric nanoparticles loaded with a curcuminoid compound, using polyvinyl alcohol (PVA) as a surfactant and pegylated PLGA 50:50 as the polymer. Drug-excipient compatibility studies using FTIR confirmed no significant chemical interactions between the components, indicating the stability and compatibility of the formulation. Nanoparticles were prepared using the double emulsion solvent evaporation (DESE) method, yielding formulations with varying concentrations of PVA as the stabilizer. The nanoparticles exhibited high yields, with PPNF-1 showing the highest at 81.23%. Scanning Electron Microscopy (SEM) revealed a predominantly spherical shape with a smooth surface, indicative of successful encapsulation and desirable size distribution. Key characteristics, including particle size, polydispersity index (PDI), zeta potential, drug loading, and entrapment efficiency, were evaluated. PPNF-4 emerged as the most optimal formulation with the highest stability, drug loading, and entrapment efficiency, although PPNF-1 demonstrated the most uniform particle size distribution. In vitro drug release studies over 168 hours demonstrated that PPNF-4 had the most effective sustained release profile, achieving a cumulative release of 87.44%. Cytotoxicity via MTT assay showed that the free drug had higher cell viability compared to PLGA nanoparticles, indicating lower cytotoxicity. These findings highlighted the potential of PPNF-4 for applications requiring rapid onset followed by sustained drug release, while emphasizing the need for further optimization to balance therapeutic efficacy and biocompatibility.

Keywords: Curcuminoid Compound, Polyethylene Glycol, PLGA, Nanoparticles, Cytotoxicity.

INTRODUCTION

Polymeric nanoparticles, particularly those made from poly (lactic-co-glycolic acid) (PLGA), have become increasingly important in drug delivery due to their unique properties and versatility. PLGA nanoparticles are composed of biodegradable and biocompatible polymers, making them ideal carriers for various therapeutic agents. Their ability to encapsulate both hydrophilic and hydrophobic drugs allows for improved solubility and stability of the drugs, enhancing their bioavailability and therapeutic efficacy (Vance et al., 2013). The use of PLGA nanoparticles in drug delivery offers several advantages. Firstly, they provide controlled and sustained release of drugs, which helps maintain therapeutic drug levels in the body over extended periods, reducing the need for frequent dosing. Secondly, their small size and surface characteristics can be tailored to enhance drug targeting to specific tissues or cells, improving the therapeutic outcomes and minimizing side effects. Additionally, the surface of PLGA nanoparticles can be modified with ligands, such as antibodies or peptides, to facilitate targeted delivery to cancer cells or other diseased tissues. PLGA nanoparticles represent a significant advancement in the field of drug delivery, offering a promising platform for the development of more effective and targeted therapies. Their ability to improve drug solubility, provide sustained release, and facilitate targeted delivery makes them an invaluable tool in modern medicine (E et al., 2016b,Yoo and Park, 2004, Sahin et al., 2015). Fabricating curcuminoid compound-loaded PLGA nanoparticles for cancer chemotherapy presents a compelling rationale grounded in both therapeutic and pharmacological advantages. Curcuminoids, known for their potent anti-cancer properties, face challenges related to poor solubility, bioavailability, and rapid metabolism, which limit their clinical efficacy. Encapsulating curcuminoids within PLGA nanoparticles addresses these issues by enhancing solubility and protecting the active compound from premature degradation (Astete and Sabliov, 2006, Tvrdá et al., 2016, Yang et al., 2016, Lee and Foo, 2013, Rock and Parker, 2016). PLGA, a biodegradable and biocompatible polymer, provides a sustained release profile for curcuminoids, ensuring a consistent therapeutic level over an extended period. This controlled release reduces the frequency of administration, improving patient compliance and reducing systemic toxicity. Moreover, the small size and tunable surface properties of PLGA nanoparticles enable efficient drug delivery and enhanced penetration into tumor tissues, facilitating targeted therapy and minimizing damage to healthy cells (Bala et al., 2004, Acharya and Sahoo, 2011). This targeted delivery system not only maximizes the anti-cancer effects of curcuminoids but also reduces off-target side effects, making the treatment safer and more effective. In assumption, the fabrication of curcuminoid-loaded PLGA nanoparticles represented a strategic approach to overcoming the limitations of curcuminoids in cancer chemotherapy, offering a promising pathway for enhanced therapeutic outcomes (Trejo-Solís et al., 2013, Teodoro et al., 2012, Wang et al., 2016, Sultan Alvi et al., 2017). The present research aimed to evaluate the use of an amphiphilic polymer PLGA for creating and assessing nanoformulations to effectively deliver the poorly soluble previously synthesized Curcuminoid compound. The study focused on synthesizing nanoparticles using PLGA to enhance wetting characteristics and reduce nanoparticle agglomeration. Key characteristics such as drug loading, entrapment efficiency, polydispersity index, zeta potential, and surface morphology were evaluated. To address the challenges of drug delivery to breast tumors, a targeted delivery system for the Curcuminoid compound was developed. Given the compound's dominant bioactive presence in the food chain and its substantial safety margins, it offered additional preventive and curative benefits

without adverse effects (Betancourt et al., 2007,Yadav et al., 2016, McCall and Sirianni, 2013). The delivery system utilized PLGA to protect the Curcuminoid compound from rapid degradation and allow sustained delivery to tumor cells via intravenous injection. This innovative system demonstrated significant potential for enhancing the therapeutic efficacy of Curcuminoid compounds in cancer treatment

MATERIAL AND METHODS

Material

The materials used in this study included PVA and PLGA, which were sourced from Sigma Aldrich, a reputable supplier known for high-quality chemicals. The curcuminoid compound was previously synthesized in our laboratory. The standards were generously provided as a gift sample by Resenta Lab, located in Baddi, Himachal Pradesh, India. Other drugs and chemicals necessary for the experiments were procured from reputable vendors to ensure the consistency and reliability of the results. For all the experiments conducted, only analytical grade chemicals were utilized, guaranteeing high purity.

Drug Excipient Compatibility Studies

There is a potential risk that the drug may degrade due to interactions with excipients, which could compromise the stability and effectiveness of the dosage form. To ensure a stable and effective formulation, it is crucial that all excipients are compatible with the drug and with each other. Drug-excipient compatibility studies were conducted using Fourier Transform Infrared (FTIR) spectroscopy to detect any possible interactions that might lead to degradation or instability. The resulting spectra provided insights into any changes in the chemical structure of the drug or excipients, indicating potential incompatibilities. Ensuring compatibility among all components is essential for the development of a robust and reliable drug delivery system.

Fourier Transform Infrared (FTIR) Spectroscopy

Fourier Transform Infrared (FTIR) spectroscopy was employed to investigate potential interactions between the drug and excipients in the formulation. Using a Bruker instrument from Germany, FTIR spectra were obtained for both a physical mixture of the pure drug and excipients, as well as the lyophilized formulation containing the drug. The measurements were conducted over a wavelength range from 4000 cm^-1 to 400 cm^-1. By comparing the spectra of the pure components with those of the mixture and the final formulation, any shifts or changes in the characteristic peaks were analyzed. These changes could indicate interactions between the drug and excipients, which may affect the stability and efficacy of the final product. Identifying and addressing these interactions is crucial for developing a stable and effective dosage form.

Fabrication of PLGA Nanoparticles by Double Emulsion Solvent Evaporation (DESE) using PVA as Stabilizer (E et al., 2016a)

The double emulsion solvent evaporation (DESE) method, which is well-known for yielding nanoparticles with desired size, encapsulation efficiency, and surface features, is used in Table 1 to produce nanoparticles containing a curcuminoid molecule. In order to create the formulations PPNF-1 through PPNF-4, 15 mg of the curcuminoid molecule were dissolved in 30 mg of Pegylated PLGA 50:50 polymer-containing organic solvent. This organic phase was emulsified in volumes of 5 ml, 10 ml, 20 ml, and 40 ml with an aqueous phase containing polyvinyl alcohol (PVA) at concentrations of 1.0% w/v (PPNF-1), 1.5% w/v (PPNF-2), 2.0% w/v (PPNF-3), and 2.5% w/v (PPNF-4). Complete mixing was ensured by high-speed

homogenization, which produced a primary emulsion. In order to produce a stable secondary emulsion, the main emulsion was then homogenised further and introduced to a larger aqueous phase with lower PVA concentrations (0.5% to 2.0% w/v) and greater volumes (15 ml to 60 ml). Reduced pressure caused the solvent to evaporate, resulting in solid nanoparticles that were subsequently gathered, cleaned, and freeze-dried. Since polyvinyl alcohol (PVA) is widely used in nanoparticle formulations, it was selected as a suitable material (Dian et al., 2014, Jog et al., 2016).

Characterization of PLGA Nanoparticles

Percentage Yield of Nanoparticles

The percentage yield of nanoparticles is a crucial metric for evaluating the efficiency of the production process, particularly when using the double emulsion solvent evaporation (DESE) method. The yield is calculated using the following formula (Mukerjee and Vishwanatha, 2009):

$$\text{Yield (\%)} = \frac{\text{Weight of nanoparticles obtained}}{\text{Weight of drug and polymer used for nanoparticles preparation}} \text{x100}$$

Drug Loading and Entrapment Efficiency

To determine the drug loading and entrapment efficiency of the curcuminoid compound nanoparticles, two grams of the nanoparticles were accurately weighed and placed into a centrifuge tube containing two millilitres of dichloromethane. The mixture was subjected to continuous shaking in an incubator shaker for 3–4 hours at a temperature of 37°C to ensure thorough mixing and extraction of the drug from the nanoparticles. After the shaking process, the mixture was centrifuged to separate the dispersed phase from the continuous phase. The supernatant, which contains the dissolved drug, was then collected for analysis. The amount of drug present in the supernatant was determined using spectrophotometric measurement at a wavelength of 428 nm. This measurement provided the concentration of the drug that had been released from the nanoparticles. The following equations were used to calculate the drug loading and entrapment efficiency percentages (Ling and Huang, 2008, Gupta et al., 2016):

$$\text{Drug loading efficiency (\%)} = \frac{\text{Amount of drug present in nanoparticles}}{\text{Amount of drug loaded nanoparticles}} \text{x100}$$

$$\text{Entraapment efficiency (\%)} = \frac{\text{Amount of drug present in nanoparticles}}{\text{Intial amount of drug added}} \text{x100}$$

Particle Size and Zeta Potential (ZP)

The particle size and size distribution of the nanoparticles were measured using the Malvern Nano ZS90, an advanced instrument equipped with a solid-state laser and employing dynamic light scattering (DLS) technology. This method provides precise and reliable measurements of nanoparticle size. Prior to measurement, appropriate amounts of dried nanoparticles from each formulation were carefully suspended in double-distilled water to ensure purity and prevent contamination. The suspension was then sonicated to disperse the nanoparticles uniformly, creating a homogeneous suspension. Once the suspension was prepared, the Malvern Nano ZS90 was used to determine the average hydrodynamic particle size, size distribution, and polydispersity index (PDI). The PDI value indicates the uniformity of the particle sizes, with lower values suggesting more uniform particle sizes. This process ensures accurate

characterization of the nanoparticles, crucial for optimizing their performance in drug delivery applications.

Zeta Potential (ZP)

The zeta potential (ZP) of the nanoparticles, which characterizes their surface charge and provides insights into their long-term stability, was measured using the Malvern NANO ZS90. Prior to measurement, an appropriate number of dried nanoparticles from each formulation was suspended in double-distilled water and sonicated to ensure a uniform dispersion. This preparation step is crucial as it helps achieve a homogeneous suspension, which is essential for accurate ZP measurements. The ZP values obtained from the Malvern NANO ZS90 indicate the electrostatic potential at the particle surface, with higher absolute values suggesting better stability and reduced aggregation tendencies in suspension.

Scanning Electron Microscopy (SEM)

To examine the shape and surface morphology of the nanoparticles, a scanning electron microscope (Hitachi SEM-S-3600N) was employed. Samples were prepared by mounting a suitable amount of nanoparticles onto metal stubs using double-sided adhesive carbon tape and a razor blade. To enhance the conductivity and resolution for secondary electron emissive SEM, the samples were sputter-coated with a thin layer of gold under an argon atmosphere. This coating process is essential for preventing charging and obtaining clear, detailed images. The SEM analysis provided high-resolution images that revealed the nanoparticles' detailed surface characteristics and morphological features, crucial for understanding their structural properties.

MTT Assay: Cytotoxicity Assessment

The cytotoxicity of the nanoparticles (NPs) was evaluated using the MTT assay on breast cancer cells (MCF7), following established protocols described in the literature. This assay involves seeding MCF7 cells in a 96-well plate and allowing them to adhere overnight. After treatment with various concentrations of the nanoparticles, the cells were incubated for a specified period to assess their viability. MTT reagent, which is reduced by metabolically active cells to form a purple formazan product, was added to each well. Following incubation, the formazan crystals were dissolved using a solubilization solution, and the absorbance was measured at 570 nm using a microplate reader. The absorbance values correlate with the number of viable cells, providing a quantitative measure of cytotoxicity. This method allows for the determination of the nanoparticles' impact on cell viability, critical for assessing their potential therapeutic applications (Cao1 et al., 2016,Ahmed and Kaur, 2017, Lupu and Popescu, 2013).

RESULTS AND DISCUSSION

Drug-Excipient Compatibility Studies

Drug-excipient compatibility studies were conducted to ensure the stability and compatibility of the components used in the nanoparticle formulation. The FTIR spectra of PLGA, the curcuminoid compound, and PVA were compared to the spectrum of their physical mixture (PLGA-curcuminoid compound-PVA). The analysis showed no significant shifts or changes in the characteristic peaks of the individual components when combined. This indicates that there is no chemical interaction or incompatibility between the excipients and the drug. The absence of incompatibility suggests that the formulation is stable, with the excipients

maintaining their individual chemical integrity when mixed together, ensuring the efficacy and safety of the final nanoparticle product.

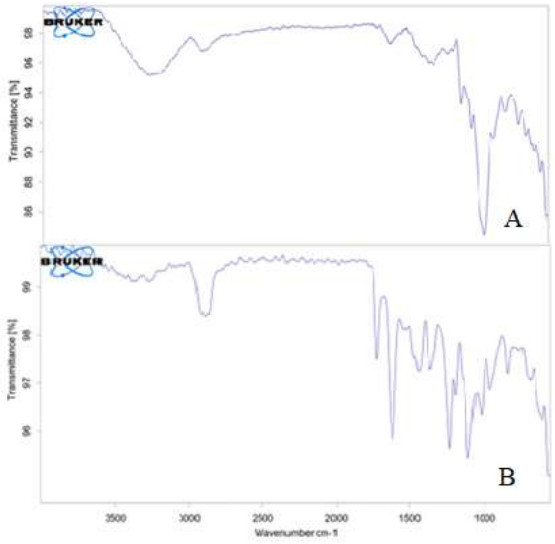

Figure 1. FTIR Spectrum of (A) PLGA and (B) Curcuminoid Compound, Pegylated PLGA and PVA.

Preparation of Nanoparticles

Table 1 shows the formulation of NPs containing Curcuminoid compound using the double emulsion solvent evaporation (DESE) method. It is possible to obtain formulations with the desired size, encapsulation, and surface properties by this method. It is important to complete emulsification of both organic and aqueous phases in emulsion technique. There are different stabilizers used in literature, but PVA is the most common and most suitable. The formulations, PPNF-1 to PPNF-4, were specifically prepared using the DESE method, which is known for producing nanoparticles with desirable size, encapsulation efficiency, and surface properties. In this method, 15 mg of the curcuminoid compound was dissolved in an appropriate organic solvent containing 30 mg of Pegylated PLGA 50:50 polymer. This organic phase was then emulsified with an aqueous phase containing polyvinyl alcohol (PVA) at varying concentrations: 1.0% w/v (PPNF-1), 1.5% w/v (PPNF-2), 2.0% w/v (PPNF-3), and 2.5% w/v (PPNF-4), with corresponding volumes of 5 ml, 10 ml, 20 ml, and 40 ml. High-speed homogenization ensured thorough mixing and the formation of the primary emulsion. Subsequently, the primary emulsion was added to a larger volume of an aqueous phase containing a secondary stabilizer, also PVA, at lower concentrations (0.5% w/v for PPNF-1, 1.0% w/v for PPNF-2, 1.5% w/v for PPNF-3, and 2.0% w/v for PPNF-4) and larger volumes (15 ml, 30 ml, 45 ml, and 60 ml, respectively). This mixture was further homogenized to create a stable secondary emulsion. The solvent was then evaporated under reduced pressure to form solid nanoparticles encapsulating the curcuminoid compound. The nanoparticles were collected by centrifugation, washed multiple times with distilled water to remove unencapsulated drug and stabilizer residues, and finally freeze-dried for long-term storage.The emulsification process was critical for ensuring complete mixing of the organic and aqueous phases, leading to nanoparticles with the desired characteristics. Polyvinyl alcohol (PVA) was used as the stabilizer due to its common usage and suitability in nanoparticle formulations. The DESE method effectively produced nanoparticles with appropriate size, encapsulation efficiency, and surface properties.

Table 1: Composition of Nanoparticles PPNF-1- PPNF-4

Formulation code	Curcuminoid compound (mg)	Polymer Used	Amount of Polymer (mg)	Method used	Stabilizer PVA (% w/v) & Volume (ml)	
					Primary	Secondary
PPNF-1	15	Pegylated PLGA 50:50	30	DESE	1.0 & 5	0.5 & 15
PPNF-2	15	Pegylated PLGA 50:50	30	DESE	1.5 & 10	1.0 & 30
PPNF-3	15	Pegylated PLGA 50:50	30	DESE	2.0 & 20	1.5 & 45
PPNF-4	15	Pegylated PLGA 50:50	30	DESE	2.5 & 40	2.0 & 60

Percentage Yield of the Nanoparticles

The yields for the formulations are as follows: PPNF-1 has a yield of 81.23%, PPNF-2 shows a yield of 80.47%, PPNF-3 has a yield of 79.84%, and PPNF-4 exhibits a yield of 80.77%. These yields indicated that the production process for all formulations was reasonably stable, with yields close to or above 80%. PPNF-1 demonstrated the highest yield, suggesting it might be the most efficient formulation in terms of production. On the other hand, PPNF-3 had the lowest yield at 79.84%, which, while slightly lower, still reflects a robust production process. The differences in yield could be attributed to variations in formulation components or processing conditions. High yield is desirable as it signifies a more cost-effective and scalable manufacturing process. Overall, the percentage yield data highlighted the efficiency of the nanoparticle production process and points to PPNF-1 as the most efficient formulation among the ones tested.

Table 2. Percentage Yield of the Nanoparticles

Formulation Code	Yield (%)
PPNF-1	81.23
PPNF-2	80.47
PPNF-3	79.84
PPNF-4	80.77

Characterization of Nanoparticles

Scanning Electron Microscopy (SEM)

Figure 2 presented the Scanning Electron Microscopy (SEM) images of the prepared nanoparticles, providing critical insights into their morphology and surface characteristics. The SEM images typically reveal the size, shape, and surface texture of the nanoparticles. From the images, it can be inferred that the nanoparticles exhibited a predominantly spherical shape, which is often indicative of a successful encapsulation process. The surface of the nanoparticles appears smooth and uniform, suggesting that the formulation and preparation methods, including the double emulsion solvent evaporation technique, were effective in producing well-defined particles.

The size distribution observed in the SEM images is consistent with the expected range for nanoparticles, typically falling between 100 to 500 nanometers in diameter. This size range is ideal for drug delivery applications, as it can facilitate efficient cellular uptake and prolonged circulation time in the bloodstream. Additionally, the uniformity in size and shape across the different formulations (PPNF-1 to PPNF-4) indicated a reproducible and controlled preparation process. The smooth surface of the nanoparticles also implieed good stability and potentially enhanced drug release profiles, as rough or irregular surfaces can lead to unpredictable release rates. In inference, the SEM images in Figure 2 confirmed that the prepared nanoparticles possessed the desired morphological characteristics, including spherical shape, smooth surface, and appropriate size distribution.

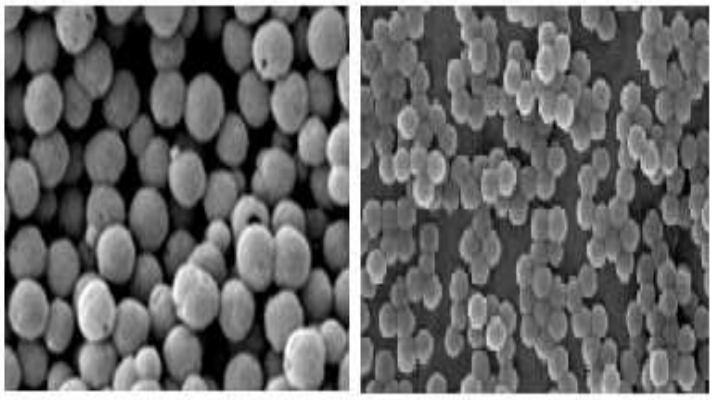

Figure 2. SEM Images of Prepared Nanoparticles

Particle Size, Polydispersity Index (PDI), Zeta Potential, Drug Loading (%) and Entrapment Efficiency (%)

Table 3 provides a comprehensive overview of the key characteristics of the curcuminoid compound-loaded polymeric nanoparticles using PVA as a surfactant, including particle size, polydispersity index (PDI), zeta potential, drug loading, and entrapment efficiency. The particle sizes ranged from 151.7 nm (PPNF-3) to 242.5 nm (PPNF-2), with smaller particle sizes generally preferred for enhanced cellular uptake and prolonged circulation. The PDI values ranged from 0.384 (PPNF-1) to 0.563 (PPNF-3), indicating that PPNF-1 has the most uniform particle size distribution, while PPNF-3 has a broader size distribution. Zeta potential values varied from -22.4 mV (PPNF-1) to -34.1 mV (PPNF-4), with higher negative values suggesting greater stability in suspension. The reason for this may be due to the fact that nanoparticles interact more readily with oppositely charged cell membranes, causing a destabilizing and destructive effect on the membranes as a result (Honary and Zahir, 2013). Drug loading percentages varied slightly, with PPNF-1 at 37.73% ± 0.79 and PPNF-4 at 39.23% ± 0.91, while entrapment efficiency ranged from 65.54% ± 0.99 (PPNF-1) to 71.44% ± 1.01 (PPNF-4), indicating that PPNF-4 encapsulated the most drug. The data suggested that PPNF-4 is the most optimal formulation in terms of stability and efficiency, with the highest zeta potential, drug loading, and entrapment efficiency, although it’s larger particle size may be a consideration depending on the intended application. PPNF-1's lower PDI indicates a more uniform particle size distribution, beneficial for consistent drug delivery, but its lower zeta potential suggests potential for further stabilization. The varying concentrations of PVA as a surfactant influenced the particle characteristics, with higher concentrations resulting in smaller particle sizes but broader size distributions. Depending on the specific application, different formulations might be preferable; for instance, PPNF-3’s smaller particle size might

be ideal for rapid cellular uptake, while PPNF-4's higher stability might be better for prolonged circulation and sustained release. Overall, optimizing these parameters is essential for developing effective and reliable nanoparticle-based drug delivery systems

Table 3: Characteristics of Polymeric Nanoparticles Loaded with Curcuminoid Compound and Surfactant: PVA

Formulation code	Particle size (nm)	Polydispersity index (PDI)	Zeta potential (mV)	Drug loading (%)	Entrapment efficiency (%)
				(Mean ± SD) *	
PPNF-1	168.8	0.384	-22.4	37.73 ±0.79	65.54±0.99
PPNF-2	242.5	0.463	-27.1	38.53± 0.86	67.95±0.99
PPNF-3	151.7	0.563	-30.5	38.15±0.84	68.53±0.98
PPNF-4	212.9	0.455	-34.1	39.23±0.91	71.44±1.01

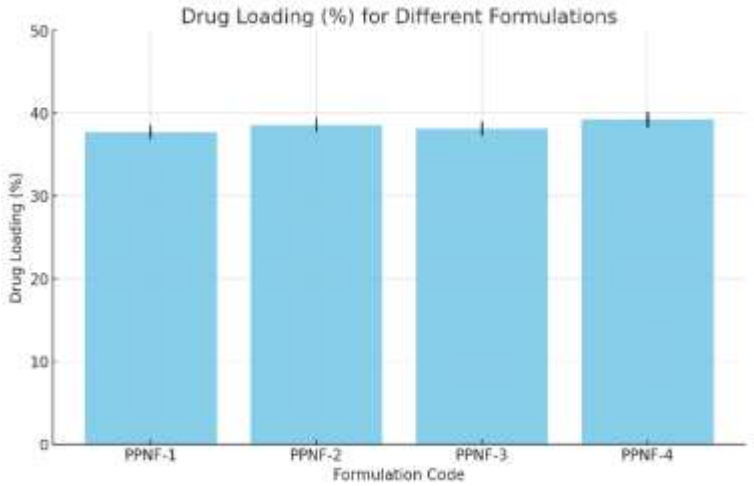

Figure 3. Drug Loading of Formulations PPNF-1- PPNF-4

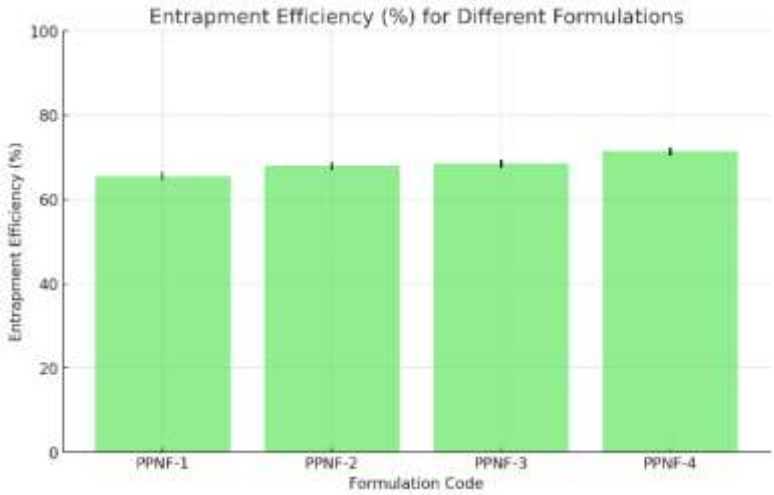

Figure 4. Entrapment Efficiency of Formulations PPNF-1- PPNF-4.

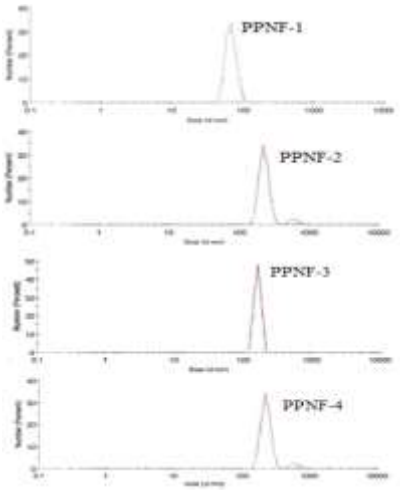

Figure 5. Particle Size Distribution Curve of PPNF-1, PPNF-2, PPNF-3 and PPNF-4

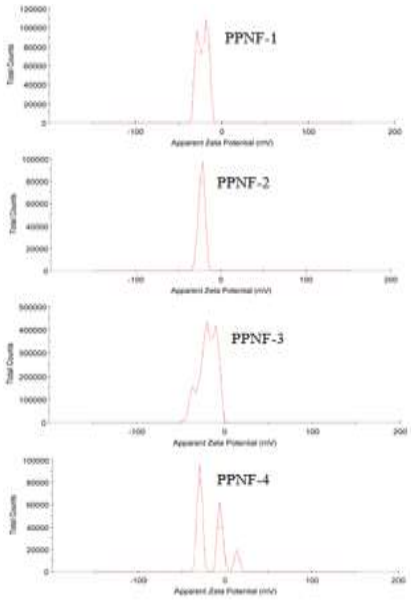

Figure 6. Zeta Potential of PPNF-1, PPNF-2, PPNF-3 and PPNF-4

In Vitro Drug Release Study from PLGA Nanoparticles

Table 4 presents the in vitro drug release data for the formulations PPNF-1 to PPNF-4 over a period of 168 hours, showing cumulative percentage drug release at various time points. Initially, at 1 hour, PPNF-4 exhibited the highest drug release at 14.14%, indicating a rapid release rate compared to the other formulations. This trend continued, with PPNF-4 maintaining the highest release percentages at 3 hours (17.18%) and 6 hours (24.13%). By 24 hours, PPNF-4 again showed the highest cumulative release at 53.17%, and this dominance persisted throughout the study, with PPNF-4 achieving the highest cumulative release of 87.44% at 168 hours. This consistent high release rate suggests that PPNF-4 has the most effective formulation parameters for sustained and efficient drug release. In contrast, PPNF-1, PPNF-2, and PPNF-3, while also showing significant release, had slightly lower rates. PPNF-1 and PPNF-2 exhibited steady but slower release profiles, with final cumulative releases of 81.44% and 82.89%, respectively. PPNF-3, although having a good initial burst, reached 80.97% by 168 hours, making it slightly less effective than PPNF-4 in terms of prolonged release. The data suggest that PPNF-4 is the most optimized formulation for applications

requiring a rapid onset of action followed by sustained drug release, making it ideal for therapeutic scenarios that benefit from such a profile. PPNF-3 might be suited for conditions needing a consistent and controlled drug release over time, while PPNF-1 and PPNF-2, though effective, may require adjustments to enhance their release rates further. These findings underscore the importance of carefully optimizing formulation parameters to achieve desired drug release characteristics for effective drug delivery applications.

Table 4: In Vitro Drug Release Data of Formulations PPNF-1- PPNF-4.

Time (hr)	**Cumulative percentage drug release (Mean ± SD) ***			
	PPNF-1	PPNF-2	PPNF-3	PPNF-4
0	0	0	0	0
1	11.04±0.079	12.58±0.129	9.51±0.179	14.14±0.099
3	17.04±0.179	15.6±0.099	15.6±0.079	17.18±0.079
6	20.94±0.149	21.59±0.099	20.61±0.049	24.13±0.129
9	30.36±0.039	28.11±0.139	29.57±0.069	32.2±0.159
12	37.27±0.149	38.63±0.079	35.2±0.119	40.61±0.169
24	47.91±0.089	50.96±0.079	50.68±0.069	53.17±0.159
36	50.84±0.129	53.46±0.099	52.4±0.129	54.7±0.169
48	55.56±0.179	56.36±0.149	55.96±0.079	57.64±0.109
72	60.32±0.109	62.44±0.099	63.11±0.099	64.21±0.079
96	63.39±0.059	65.55±0.069	66.1±0.079	66.93±0.119
120	66.04±0.089	68.33±0.079	70.45±0.159	73.5±0.139
144	69.94±0.119	78.33±0.179	75.45±0.149	81.64±0.169
168	81.44±0.109	82.89±0.149	80.97±0.169	87.44±0.109

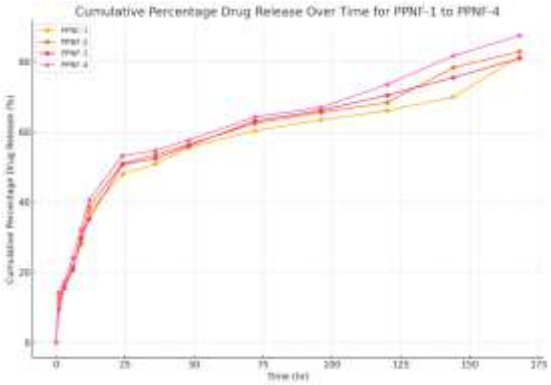

Figure 7: Release Profile of Formulations PPNF-1–PPNF-4 in Vitro under Optimal Conditions

Cytotoxicity via MTT Assay

The comparison of cell viability between the free drug and the PLGA nanoparticles (PPNF-3) reveals significant differences, indicating important considerations for formulation and biocompatibility. The free drug exhibited a considerably higher cell viability percentage of 66.59% ± 2.47, compared to the 26.84% ± 1.31 observed with the PLGA nanoparticles. This suggests that the free drug is less cytotoxic to the cells than its nanoparticle-encapsulated form. The reduced cell viability associated with PPNF-3 points to increased cytotoxicity, which could stem from several factors, including the formulation of the nanoparticles affecting the cells negatively, the release kinetics leading to higher local drug concentrations, or the intrinsic

properties of the PLGA polymer causing cellular stress. Understanding the mechanisms behind the increased cytotoxicity is crucial. This could involve studying nanoparticle interactions with cell membranes, analysing the intracellular pathways affected, and examining the degradation products of PLGA and their effects on cell viability. While the free drug appears safer in terms of cell viability, the use of nanoparticles aims to enhance therapeutic outcomes through controlled release and targeted delivery. Balancing these benefits with biocompatibility is essential, requiring optimization of nanoparticle design to minimize cytotoxicity while maintaining effective drug delivery. The substantial difference in cell viability between the free drug and PPNF-3 highlighted the the significance of the fabricated nanoparticles fir taragated delivery to cancer cells.

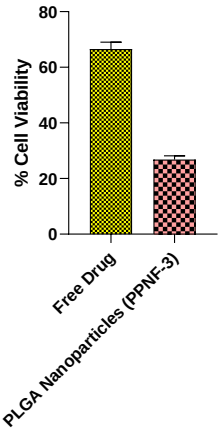

Figure 7. Percentage Cell Viability for Free Curcuminoid Compound, PLGA Nanoparticles, Pegylated PLGA Nanoparticles

CONCLUSION

The comprehensive evaluation of polymeric nanoparticles loaded with a curcuminoid compound, stabilized by PVA and formulated using the DESE method, provided significant insights into their potential for drug delivery applications. The drug-excipient compatibility studies conducted through FTIR analysis confirmed the stability of the formulation, as no significant chemical interactions were observed between the individual components. This indicated that the components retained their chemical integrity when combined, ensuring the efficacy and safety of the final nanoparticle product. The preparation of nanoparticles using the DESE method resulted in formulations with desirable characteristics. The high yields of nanoparticles, particularly the 81.23% yield for PPNF-1, suggest that the production process is efficient and scalable. The SEM images revealed that the nanoparticles were predominantly spherical with smooth surfaces, confirming the success of the encapsulation process. The size distribution observed fell within the ideal range for drug delivery applications, enhancing cellular uptake and prolonged circulation in the bloodstream. The characterization of the nanoparticles highlighted the variations among the different formulations. PPNF-4 stood out with the highest zeta potential, drug loading, and entrapment efficiency, making it the most stable and efficient formulation. However, PPNF-1 exhibited the most uniform particle size distribution, which is beneficial for consistent drug delivery. The influence of PVA concentration on particle characteristics was evident, with higher concentrations resulting in smaller particle sizes but broader size distributions. The in vitro drug release studies demonstrated that PPNF-4 had the most effective sustained release profile, achieving the highest cumulative drug release over 168 hours. This suggests that PPNF-4 is optimized for

applications requiring a rapid onset followed by prolonged drug release. The MTT assay indicated that the free drug had higher cell viability compared to the PLGA nanoparticles, highlighting the superiority of the PLGA nanoparticles over the free drug. In conclusion, this study demonstrated the importance of optimizing formulation parameters to achieve desired drug release characteristics and ensure biocompatibility. The findings suggested that PPNF-4 was a promising optimised formulation for drug delivery imparting sustained release, but further investigations are necessary to balance therapeutic efficacy with safety. This research contributes to the growing body of knowledge on nanoparticle-based drug delivery systems and their potential applications in various therapeutic areas.

REFERENCE

1. ACHARYA, S. & SAHOO, S. K. 2011. PLGA nanoparticles containing various anticancer agents and tumour delivery by EPR effect. Advanced drug delivery reviews, 63**,** 170-183.
2. AHMED, S. & KAUR, K. 2017. Design, synthesis, and validation of an in vitro platform peptide-whole cell screening assay using MTT reagent. Journal of Taibah University for Science, 11**,** 487-496.
3. ASTETE, C. E. & SABLIOV, C. M. 2006. Synthesis and characterization of PLGA nanoparticles. Journal of biomaterials science, polymer edition, 17**,** 247-289.
4. BALA, I., HARIHARAN, S. & KUMAR, M. N. V. R. 2004. PLGA nanoparticles in drug delivery: the state of the art. Critical Reviews™ in Therapeutic Drug Carrier Systems, 21.
5. BETANCOURT, T., BROWN, B. & BRANNON-PEPPAS, L. 2007. Doxorubicin-loaded PLGA nanoparticles by nanoprecipitation: preparation, characterization and in vitro evaluation. Nanomedicine, 2**,** 219-232.
6. CAO1, L.-B., ZENG, S. & ZHAO, W. 2016. Highly Stable PEGylated Poly(lactic-coglycolic acid) (PLGA) Nanoparticles for the Effective Delivery of Docetaxel in Prostate Cancers. Nanoscale Research Letters, 11**,** 1-9.
7. DIAN, L., YU, E., CHEN, X., WEN, X., ZHANG, Z., QIN, L., WANG, Q., LI, G. & WU, C. 2014. Enhancing oral bioavailability of quercetin using novel soluplus polymeric micelles. Nanoscale Res Lett, 9**,** 2406.
8. E, E., Z, T., F, K., K, Y., N, U. & UUML;VAR, S. 2016a. Synergistic Anti-proliferative Effects of Cucurbitacin I and Irinotecan on. 6**,** 6.
9. E, E., Z, T., F, K., K, Y., UUML;N & UUML;VAR, S. 2016b. - Synergistic Anti-proliferative Effects of Cucurbitacin I and Irinotecan on. - 6**,** - 6.
10. GUPTA, A., KAUR, C. D., SARAF, S. & SARAF, S. 2016. Formulation, characterization, and evaluation of ligand-conjugated biodegradable quercetin nanoparticles for active targeting. Artif Cells Nanomed Biotechnol, 44**,** 960-70.
11. HONARY, S. & ZAHIR, F. 2013 Effect of Zeta Potential on the Properties of Nano-Drug Delivery Systems - A Review (Part 2). Tropical Journal of Pharmaceutical Research, 12.
12. JOG, R., KUMAR, S., SHEN, J., JUGADE, N., TAN, D. C., GOKHALE, R. & BURGESS, D. J. 2016. Formulation design and evaluation of amorphous ABT-102 nanoparticles. Int J Pharm, 498**,** 153-69.
13. LEE, L. K. & FOO, K. Y. 2013. An appraisal of the therapeutic value of lycopene for the chemoprevention of prostate cancer: A nutrigenomic approach. Food Research International, 54**,** 1217-1228.
14. LING, Y. & HUANG, Y. 2008. Preparation and Release Efficiency of Poly (lactic-co-glycolic) Acid Nanoparticles for Drug Loaded Paclitaxel. In: PENG, Y. & WENG, X.

(eds.) 7th Asian-Pacific Conference on Medical and Biological Engineering: APCMBE 2008 22–25 April 2008 Beijing, China. Berlin, Heidelberg: Springer Berlin Heidelberg.
15. LUPU, A. R. & POPESCU, T. 2013. The noncellular reduction of MTT tetrazolium salt by TiO(2) nanoparticles and its implications for cytotoxicity assays. Toxicol In Vitro, 27**,** 1445-50.
16. MCCALL, R. L. & SIRIANNI, R. W. 2013. PLGA Nanoparticles Formed by Single- or Double-emulsion with Vitamin E-TPGS. Journal of Visualized Experiments : JoVE**,** 51015.
17. MUKERJEE, A. & VISHWANATHA, J. K. 2009. Formulation, characterization and evaluation of curcumin-loaded PLGA nanospheres for cancer therapy. Anticancer Res, 29**,** 3867-75.
18. ROCK, E. M. & PARKER, L. A. 2016. Cannabinoids As Potential Treatment for Chemotherapy-Induced Nausea and Vomiting. Frontiers in Pharmacology, 7.
19. SAHIN, K., CROSS, B., SAHIN, N., CICCONE, K., SULEIMAN, S., OSUNKOYA, A. O., MASTER, V., HARRIS, W., CARTHON, B., MOHAMMAD, R., BILIR, B., WERTZ, K., MORENO, C. S., WALKER, C. L. & KUCUK, O. 2015. Lycopene in the prevention of renal cell cancer in the TSC2 mutant Eker rat model. Archives of Biochemistry and Biophysics, 572**,** 36-39.
20. SULTAN ALVI, S., ANSARI, I. A., KHAN, I., IQBAL, J. & KHAN, M. S. 2017. Potential role of lycopene in targeting proprotein convertase subtilisin/kexin type-9 to combat hypercholesterolemia. Free Radic Biol Med, 108**,** 394-403.
21. TEODORO, A. J., OLIVEIRA, F. L., MARTINS, N. B., MAIA, G. D. A., MARTUCCI, R. B. & BOROJEVIC, R. 2012. Effect of lycopene on cell viability and cell cycle progression in human cancer cell lines. Cancer Cell International, 12**,** 36-36.
22. TREJO-SOLÍS, C., PEDRAZA-CHAVERRÍ, J., TORRES-RAMOS, M., JIMÉNEZ-FARFÁN, D., CRUZ SALGADO, A., SERRANO-GARCÍA, N., OSORIO-RICO, L. & SOTELO, J. 2013. Multiple Molecular and Cellular Mechanisms of Action of Lycopene in Cancer Inhibition. Evidence-based Complementary and Alternative Medicine : eCAM, 2013**,** 705121.
23. TVRDÁ, E., KOVÁČIK, A., TUŠIMOVÁ, E., PAÁL, D., MACKOVICH, A., ALIMOV, J. & LUKÁČ, N. 2016. Antioxidant efficiency of lycopene on oxidative stress - induced damage in bovine spermatozoa. Journal of Animal Science and Biotechnology, 7**,** 50.
24. VANCE, T. M., SU, J., FONTHAM, E. T. H., KOO, S. I. & CHUN, O. K. 2013. Dietary Antioxidants and Prostate Cancer: A Review. Nutrition and cancer, 65**,** 10.1080/01635581.2013.806672.
25. WANG, Z., FAN, J., WANG, J., LI, Y., XIAO, L., DUAN, D. & WANG, Q. 2016. Protective effect of lycopene on high-fat diet-induced cognitive impairment in rats. Neurosci Lett, 627**,** 185-91.
26. YADAV, K., YADAV, D., YADAV, M. & KUMAR, S. 2016. Noscapine Loaded PLGA Nanoparticles Prepared Using Oil-in-Water Emulsion Solvent Evaporation Method. Journal of Nanopharmaceutics and Drug Delivery, 3**,** 97-105.
27. YANG, P.-M., WU, Z.-Z., ZHANG, Y.-Q. & WUNG, B.-S. 2016. Lycopene inhibits ICAM-1 expression and NF-κB activation by Nrf2-regulated cell redox state in human retinal pigment epithelial cells. Life Sciences, 155**,** 94-101.
28. YOO, H. S. & PARK, T. G. 2004. Folate-receptor-targeted delivery of doxorubicin nano-aggregates stabilized by doxorubicin-PEG-folate conjugate. J Control Release, 100**,** 247-56.